Comparison of Load Models for Estimating Electrical Efficiency in DC Microgrids

Preprint

A. Santos,[1] J. Cale,[1] A. Othee,[1] D. Gerber,[2] S. Frank,[3] G. Duggan,[1] D. Zimmerle,[1] and R. Brown[2]

1 Colorado State University
2 Lawrence Berkeley National Laboratory
3 National Renewable Energy Laboratory

Presented at the IEEE International Conference on DC Microgrids (ICDCM 2019)
Matsue, Japan
May 20-23, 2019

NREL is a national laboratory of the U.S. Department of Energy
Office of Energy Efficiency & Renewable Energy
Operated by the Alliance for Sustainable Energy, LLC

This report is available at no cost from the National Renewable Energy Laboratory (NREL) at www.nrel.gov/publications.

Contract No. DE-AC36-08GO28308

Conference Paper
NREL/CP-3500-77228
September 2020

Comparison of Load Models for Estimating Electrical Efficiency in DC Microgrids

Preprint

A. Santos,[1] J. Cale,[1] A. Othee,[1] D. Gerber,[2] S. Frank,[3] G. Duggan,[1] D. Zimmerle,[1] and R. Brown[2]

1 Colorado State University
2 Lawrence Berkeley National Laboratory
3 National Renewable Energy Laboratory

Suggested Citation
Santos, A., J. Cale, A. Othee, D. Gerber, S. Frank, G. Duggan, D. Zimmerle, and R. Brown. 2020. *Comparison of Load Models for Estimating Electrical Efficiency in DC Microgrids: Preprint*. Golden, CO: National Renewable Energy Laboratory. NREL/CP-3500-77228. https://www.nrel.gov/docs/fy20osti/77228.pdf.

© 2019 IEEE. Personal use of this material is permitted. Permission from IEEE must be obtained for all other uses, in any current or future media, including reprinting/republishing this material for advertising or promotional purposes, creating new collective works, for resale or redistribution to servers or lists, or reuse of any copyrighted component of this work in other works.

NREL is a national laboratory of the U.S. Department of Energy
Office of Energy Efficiency & Renewable Energy
Operated by the Alliance for Sustainable Energy, LLC

This report is available at no cost from the National Renewable Energy Laboratory (NREL) at www.nrel.gov/publications.

Contract No. DE-AC36-08GO28308

Conference Paper
NREL/CP-3500-77228
September 2020

National Renewable Energy Laboratory
15013 Denver West Parkway
Golden, CO 80401
303-275-3000 • www.nrel.gov

NOTICE

This work was authored in part by the National Renewable Energy Laboratory, operated by Alliance for Sustainable Energy, LLC, for the U.S. Department of Energy (DOE) under Contract No. DE-AC36-08GO28308. Funding provided by the U.S. Department of Energy Office of Energy Efficiency and Renewable Energy Building Technologies Office. The views expressed herein do not necessarily represent the views of the DOE or the U.S. Government. The U.S. Government retains and the publisher, by accepting the article for publication, acknowledges that the U.S. Government retains a nonexclusive, paid-up, irrevocable, worldwide license to publish or reproduce the published form of this work, or allow others to do so, for U.S. Government purposes.

This report is available at no cost from the National Renewable Energy Laboratory (NREL) at www.nrel.gov/publications.

U.S. Department of Energy (DOE) reports produced after 1991 and a growing number of pre-1991 documents are available free via www.OSTI.gov.

Cover Photos by Dennis Schroeder: (clockwise, left to right) NREL 51934, NREL 45897, NREL 42160, NREL 45891, NREL 48097, NREL 46526.

NREL prints on paper that contains recycled content.

Comparison of Load Models for Estimating Electrical Efficiency in DC Microgrids

A. Santos[1], J. Cale[1], A. Othee[1], D. Gerber[2], S. Frank[3], G. Duggan[1], D. Zimmerle[1], and R. Brown[2]

[1]Colorado State University
[2]Lawrence Berkeley National Laboratory
[3]National Renewable Energy Laboratory

***Abstract*—This paper compares several electrical load models for estimating the efficiency of DC vs. AC distribution in microgrids. Candidate models include energy balance, harmonic power flow, and time-domain modeling. Model results are compared with numerical studies and validated with experimental measurements. Based on quantitative and qualitative considerations, the most appropriate load modeling approach for larger-scale DC distribution efficiency studies is proposed.**

***Index Terms*—DC distribution, microgrids, electrical efficiency, load modeling**

I. Introduction

In recent years, there has been considerable interest in comparing the efficiency of DC distribution systems versus traditional AC distribution. This interest is inspired by an increasing proportion of residential electrical loads, miscellaneous electrical loads (MELs), and building equipment which can operate from DC distribution systems. In addition, many renewable power generation systems such as solar photovoltaic (PV) and energy storage systems natively produce DC power, making conversions between AC and DC potentially unnecessary and a possible source of energy savings [1]–[10].

Microgrid applications may particularly benefit from the advantages derived from DC distribution. Microgrids self-generate and consume their own power, making energy efficiency a high priority. These systems typically use renewable and storage systems which provide DC power. Moreover, in many microgrid applications—particularly remote or rural microgrids—electrical loads are often dominated by DC plug loads and LED lighting, making DC distribution a seemingly beneficial choice [11], [12].

However, quantifying the efficiency and life-cycle cost of competing distribution systems including AC-only, DC-only, and hybrid AC/DC can be challenging because of the number of possible electrical configurations, how system boundaries are defined, whether the application includes on-site storage and/or solar PV, and combinations of potential loads and equipment types [3], [13]. To address this need, the authors are developing next-generation modeling tools to provide a flexible and modular modeling environment to enable microgrid practitioners to assess and compare the energy efficiency and life-cycle cost of competing electrical network designs.

A key component of this research is the development and validation of electrical load models to evaluate electrical losses, underlying the comparison between competing network designs. Energy efficiency comparisons in the future integrated modeling tool are expected to be made over a wide range of potential configurations, requiring a trade-off between computational efficiency and sufficient model accuracy. To this end, this paper describes evaluations which were conducted between three modeling approaches: energy balance from device efficiency curves, a harmonic power flow method, and time-domain simulation. Modeling results were compared to measurements taken on an experimental testbed and used to down-select the most appropriate method given the dual objectives of computational speed and sufficient accuracy, in addition to scalability and ease of modeling implementation.

Research in [1], [2] described numerical comparisons between AC and DC distribution networks in residential and commercial buildings, respectively, using parameterized efficiency curves for each device, from which net power losses were calculated. Harmonic power flow is a well-established analysis technique used to estimate power flows in systems which include nonlinear loads [14], [15]. The iterative harmonic power flow technique has been shown to account for nonlinear loads, voltage distortions and can accurately model losses based on harmonics in the system, and can be used for unbalanced systems [16], [17]. Time-domain methods have been used extensively to simulate power flows and electromagnetic transients in power systems and power electronic devices, see for example [18], [19].

This paper focuses on the evaluation and comparison of the three load modeling approaches mentioned above, with primary consideration placed on down-selecting a method which yields sufficient accuracy while maintaining computational efficiency, ease of use and modeling implementation. Key contributions of this work are:

- Evaluation of several load modeling options for the assessment of DC and AC network efficiencies;
- Description of an experimental testbed and data collection method for obtaining measurements on various distribution types and configurations;
- Assessment of the load modeling approaches described above in terms of their appropriateness for use in an integrated modeling package.

The remainder of this paper is structured as follows. Sec-

This report is available at no cost from the National Renewable Energy Laboratory at www.nrel.gov/publications.

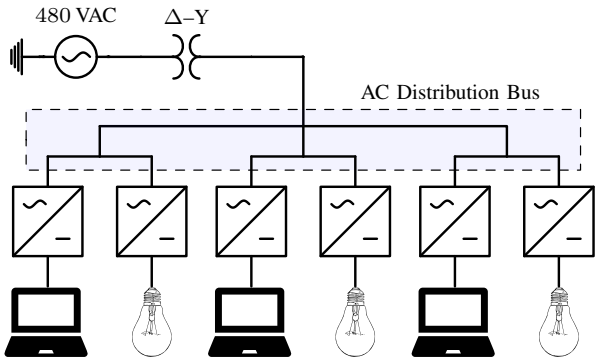

(a) AC-only distribution.

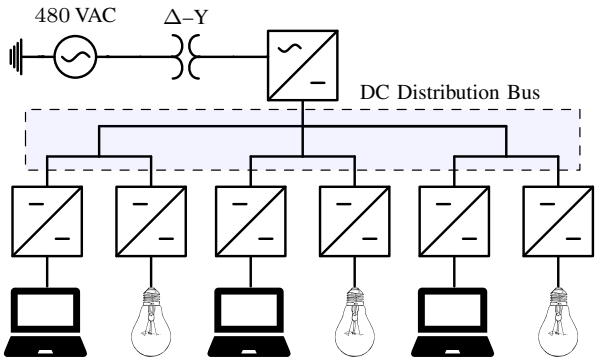

(b) DC-only distribution.

Fig. 1. Testbed configurations with AC-only (a) and DC-only (b).

tion II outlines the technical approach used in this work. Background on the selection of candidate load models is given in section III. Section IV provides a description of the experimental testbed. Model validation results are presented in section V, followed by conclusions in section VI.

II. Technical Approach

The objective of this research was to perform both quantitative and qualitative comparisons of electrical load models to determine their suitability for integration into a modeling package when considering: computational efficiency, accuracy, and ease-of-implementation. The steps used to perform these comparisons were as follows:

1) *Testbed design*. A testbed for emulating actual operating conditions in building distribution systems under both AC and DC configurations was designed.
2) *Selection of candidate load models*. Candidate load models were chosen from a set of well-known techniques, representing a spectrum of expected accuracy, computational efficiency, and implementation effort.
3) *Modeling and simulation*. Models were created for each device and network configuration in the testbed to perform estimations of electrical efficiencies.
4) *Experimental measurement*. The testbed was constructed and measurements were collected under a variety of operating scenarios and test configurations.
5) *Model validation*. The experimental measurements were compared to simulation results to validate the device- and system-level efficiency estimations.
6) *Model assessment*. The candidate models were assessed in terms of relative accuracy, computational efficiency, and implementation burden.

For the first step, a testbed was designed to emulate the loads in a small office, supplied by either AC or DC distribution. A conceptual representation of the testbed is shown in Fig. 1.

A one-line diagram of the testbed with AC distribution is shown in Fig. 1a. The configuration comprises a 3-ϕ AC building transformer with three parallel load branches; each branch may be connected to a single phase or multiple phases as described below. The primary side of the transformer, which is connected in Δ-Y, is tied to utility mains. Each load branch consists of a computer laptop with AC/DC power supply, in parallel with light emitting diode (LED) light fixture, supplied by an AC/DC driver. The DC configuration of the testbed, shown in Fig. 1b, consists of an AC building transformer (the same transformer as in Fig. 1a) with three parallel DC-only load branches. The output voltage of the transformer is converted to DC voltage with an AC/DC converter, which powers the DC distribution bus. Each load branch consists of a computer laptop and LED (the same devices in Fig. 1a); however, in this configuration the computer power supplies and LEDs are supplied by DC/DC converter types.

To consider both balanced and unbalanced loading conditions on the distribution systems, the testbed was designed to supply the loads under the configurations shown in Table I. A detailed description of the testbed hardware and equipment specifications are given in section IV.

TABLE I. Load configurations for AC and DC distribution tests.

Configuration 1: balanced across three phases			
	Phase A	**Phase B**	**Phase C**
Laptop 1	✓		
Laptop 2		✓	
Laptop 3			✓
LED 1	✓		
LED 2		✓	
LED 3			✓
Configuration 2: unbalanced on one phase			
	Phase A	**Phase B**	**Phase C**
Laptop 1	✓		
Laptop 2	✓		
Laptop 3	✓		
LED 1	✓		
LED 2	✓		
LED 3	✓		
Configuration 3: unbalanced on two phases			
	Phase A	**Phase B**	**Phase C**
Laptop 1		✓	
Laptop 2		✓	
Laptop 3			✓
LED 1		✓	
LED 2		✓	
LED 3			✓

This report is available at no cost from the National Renewable Energy Laboratory at www.nrel.gov/publications.

III. Selection of Load Modeling Approaches

When choosing candidates for modeling electrical loads, many potential techniques and their modifications could have been selected. In this research three techniques were selected for comparison, with the objective of representing a broad spectrum of expected model accuracy, computational efficiency, and implementation effort. A brief description of the selected modeling approaches is given below.

Notation: In this paper, $\tilde{X} = X\angle\theta$ denotes the phasor for sinusoidal variable $x(t) = \sqrt{2}\,X\cos(\omega t + \theta)$ (note that X is the root-mean-square of $x(t)$); $|\cdot|$ symbolizes the absolute value of a complex number or cardinality of a set; $\mathbb{R}_e\{\cdot\}$ symbolizes the real part of a complex number; $\{\cdot\}^*$ denotes complex conjugation.

A. Energy Balance

The energy balance model determines output power and power loss at each power conversion stage (device) in the network using efficiency curves. The efficiency curves are generated using experimental measurement data, taken in increments of 10% of rated power, with linear interpolation between points as described in [2]. Example efficiency curves for a set of low voltage LED drivers is shown in Fig. 2.

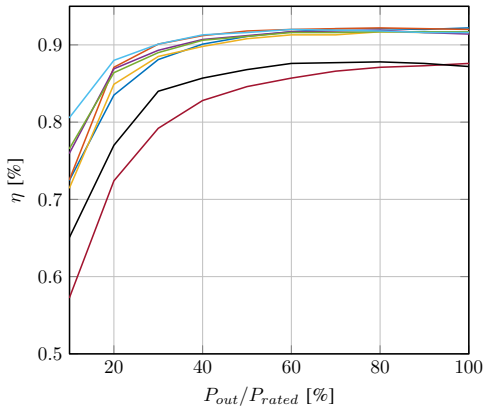

Fig. 2. Efficiency curves for low voltage LED rectifiers [2].

B. Harmonic Power Flow

The second modeling technique selected for comparison was based on harmonic power flow [14]. In this method, the electrical network is modeled in the frequency domain using a linear network at each frequency of interest; in this work, DC (0 Hz), AC fundamental (60 Hz), and odd harmonic multiples $h = 1, 3, \ldots, 19$ of the fundamental were used. In this model, power electronic converters are assumed to transfer power between linear networks; these power transfers are modeled with auxiliary equations for energy balance, converter losses, and injected harmonic currents [3].

Branch elements such as transformers and cables are represented by their standard frequency-domain models. (In the experimental testbed there was only a single branch element: a three-phase transformer.) Higher-order effects, such as nonlinear magnetizing current due to transformer saturation, are neglected. To accommodate unbalanced loads, the AC linear network at each frequency is modeled as a set of sequence networks using the theory of symmetrical components [20].

Power electronics converter losses are modeled as a quadratic function of the converter output power:

$$P_{in} = P_{out} + \underbrace{\left(\alpha + \beta P_{out} + \gamma P_{out}^2\right)}_{P_{loss}} + P_h, \qquad (1)$$

where P_{in} is the input power (DC for an inverter and AC fundamental for a rectifier); P_{out} is the output power (AC fundamental for an inverter and DC for a rectifier); P_{loss} is converter internal loss; $\alpha \in \mathbb{R}_+$, $\beta \in \mathbb{R}$, $\gamma \in \mathbb{R}$ are fitted coefficients of the loss model; P_h is a balancing term that represents power injected at harmonic frequencies. Note that neglecting P_h in (1) is equivalent to the loss model described in research published by Sandia National Laboratories, where the voltage correction terms are omitted [21], [22].

For simplicity, harmonic currents injected by power electronics converters are modeled assuming the current waveform has a fixed shape, i.e., the waveform may scale but its basic shape is invariant to power level or line voltage distortion. This fixed wave shape implies a fixed harmonic reference spectrum, which is then shifted in amplitude and phase to maintain the correct converter power input and output with respect to the voltage at the converter's AC terminal. Herein, two methods were investigated for defining the reference spectra:

1) *Single reference waveform*: For a single device, a representative waveform was captured from a single cycle during steady-state operation; its reference harmonic spectrum was obtained using the Fast Fourier Transform (FFT).
2) *Generalized impedance model*: Several waveform captures were obtained for a set of similar devices and processed using FFT. From these measurements, 5th-order polynomials were used to fit the odd harmonic magnitude and unwrapped phase angle relative to the fundamental, as a function of harmonic number. The choices of including only odd harmonic content, the maximum harmonic number, and degree of polynomial fit were based on observation of fits to measured waveforms.

The reference waveform method requires less data to implement and is potentially more accurate for the specific converter used to obtain the reference waveform. However, the frequency-domain model is more readily generalized to represent typical injection spectra expected from a broad range of similar converter types and load levels, i.e., parameterized over a catalog of device types. An example plot using the latter approach is shown in Fig. 3, which shows the harmonic current injection spectrum of an 24 V LED driver.

Herein, only radial networks were considered, from which a forward/backward sweep algorithm was used to obtain convergence in computed power flows [23]. The forward sweep used Kirchoff's voltage law (KVL) to calculate node voltages; the backward sweep used Kirchoff's current law (KCL) to calculate branch currents. In between forward and backward sweeps, the algorithm calculates injected currents from the power converters. These steps are summarized as:

This report is available at no cost from the National Renewable Energy Laboratory at www.nrel.gov/publications.

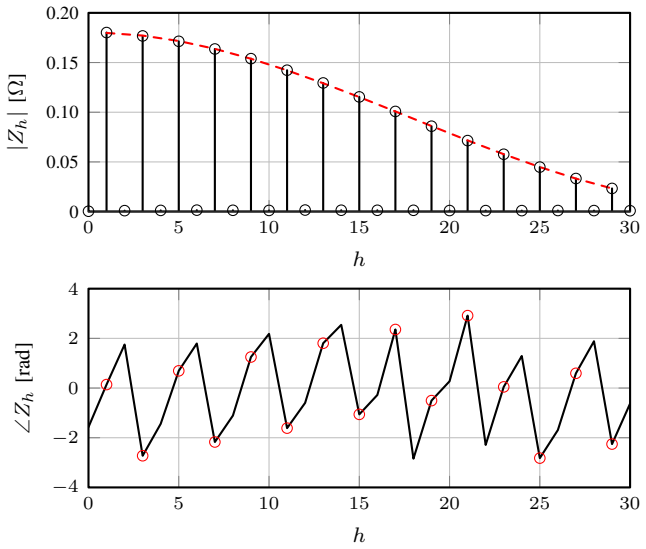

Fig. 3. Modeled harmonic current injection spectrum for 24 V LED driver. Measurements are shown in black; fitted values are shown in red.

Harmonic Power Flow Algorithm Steps:

1. Initialize voltage at input node (e.g., grid connection).
2. Calculate sequence voltages at each node via KVL, using most recent estimates of branch current.
3. Transform sequence voltages to phase voltages.
4. Using the phase voltages and known values for P_{out}, calculate rectifier currents and compute P_{in} by shifting and scaling the reference spectra ensure the:
   a) rectifier fundamental frequency AC current phase angle is correct with respect to voltage phase angle;
   b) AC real power at fundamental frequency equals P_{in};
   c) power balance in (1) is satisfied;
   d) harmonic power equals the sum of powers injected at each harmonic frequency, i.e.,

$$P_h = \sum_h \mathbb{R}_e\{\tilde{V}_h \tilde{I}_h^*\} \tag{2}$$

5. Transform load phase currents to sequence currents.
6. Calculate sequence currents in each branch via KCL using load sequence currents and most recent estimates of node voltage.
7. If not converged, return to step 2.

Steps 2-7 of the above algorithm are iterated until both the real and reactive power consumption at the source node (the electric grid) converge within a specified tolerance. In this work, a tolerance of 0.01 VA was used.

C. Time-Domain Modeling

Time-domain modeling of power electronics and systems is well-described in the literature. While time-domain modeling can often be used to obtain a high level of accuracy, it poses several drawbacks including: more effort to derive higher-fidelity models, the need to identify a larger number of model parameters, and comparatively long simulation times. However, time-domain modeling was compared to the methods described above to (*i*) compare simulation times versus accuracy, (*ii*) indicate the modeling effort required to perform full time-domain simulation, (*iii*) provide a further check on the simulation accuracy of the previous approaches.

The devices which were modeled in this research included: a three-phase AC transformer, AC/DC converter, computer power supplies (AC/DC and DC/DC types), and LED drivers (AC/DC and DC/DC types). The AC transformer was modeled using the standard equivalent circuit representation of a symmetrical (i.e., identical parameter values on each phase) 3-ϕ transformer [19]. Parameters for the transformer model used in this work are tabulated in the Appendix.

The AC/DC power electronic converters in the studies were all modeled with the same topology, employing a single-phase line-commutated diode rectifier preceding a voltage controlled DC/DC ("buck") converter, which is a simplified version of circuits commonly used in these converters. This converter is depicted in Fig. 4.

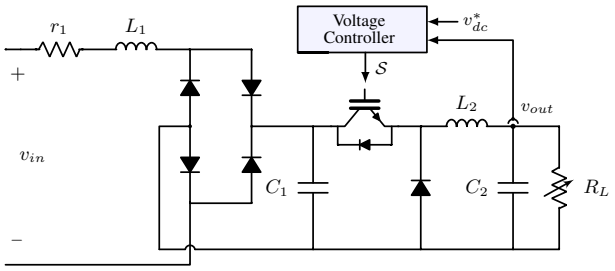

Fig. 4. Diagram of AC/DC power converter.

In Fig. 4, r_1 and L_1 are the line resistance and inductance of the input wire respectively; C_1 and C_2 are filter capacitors; L_2 is a filter inductor, and R_L is the variable equivalent load resistance. Feedback control of the converter was modeled using proportional integral (PI) control with proportional and integral gains k_p and k_i, respectively; switching state $\mathcal{S}$ varies the switch duty cycle using pulse-width-modulation with sawtooth period T_s to minimize the error between the measured output voltage v_{out} and commanded voltage reference v_{dc}^* as described in [18]. Circuit and control parameters associated with Fig. 4 for each AC/DC device used in this research are tabulated in the Appendix.

The DC/DC power converters were all modeled with the same assumed topology, employing a voltage controlled "boost" converter. This circuit is shown in Fig. 5.

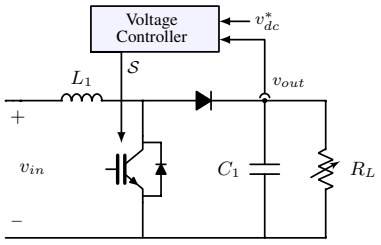

Fig. 5. Diagram of DC/DC power converter.

This report is available at no cost from the National Renewable Energy Laboratory at www.nrel.gov/publications.

In Fig. 5, L_1 is a line filter inductance, C_1 is a filter capacitor, and R_L is the variable equivalent load resistance. Feedback control of the converter was implemented with a PI loop in the same manner described for the buck converter. Circuit and control parameters associated with Fig. 5 for each DC/DC device used in this research are given in the Appendix.

To avoid modeling specific DC isolation methods and/or conflicts in the feedback control between the central distribution and load converters, the DC distribution network configuration employed virtual isolation between the distribution bus output and load inputs.

IV. Experimental Testbed

To evaluate the candidate modeling approaches described in section II under DC-only and AC-only power distribution scenarios, a testbed was constructed at the Powerhouse Energy Campus at Colorado State University. The testbed was designed to emulate realistic loads found in a small office building, comprising three laptop computers and three LED lighting systems on each load branch (refer to Fig. 1).

A. Testbed Hardware

The testbed was constructed using industrial-grade electrical equipment, mounted on a panel-board for convenience during configuration changes and access to measurement points, see Fig. 6. To implement the configuration scenarios listed in Table I and provide circuit protection, the electrical enclosure ("load center") in Fig. 6 contained DIN-rail mounted switches and fuse boxes, supplying a total of six possible load branches.

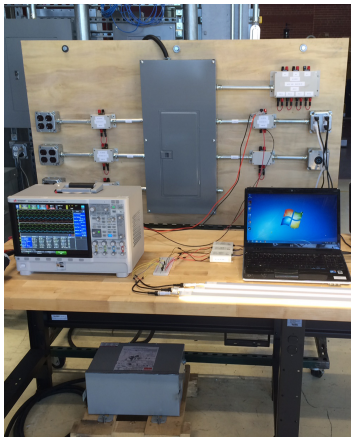

Fig. 6. Testbed hardware with power analyzer, laptop, and LEDs. *(Photo used with permission by Arthur Santos of Colorado State University.)*

The load center was connected to utility mains through a 3 kVA, Δ-Y transformer (Dayton model 44YV25), with 480 V primary and 208 V/120 V secondary. Electrical outlets on each load branch provided a total of 16 outlets for single-phase 120 V, and two for three-phase 208 V. Each branch was protected from over-current with a 10 A circuit breaker.

The laptop computers used in the experiments and their power supplies consisted of:

Laptop 1: HP notebook, model Envy dv6-7210us, with AC/DC converter model 677774-001 (65 W), and DC/DC converter model HP F1455A Airline/Auto Adapter (75 W)

Laptop 2: HP notebook, model Elitebook 850 G3, with AC/DC converter model 740015-002 (45 W), and DC/DC converter model PA-3900-Z3 (90 W)

Laptop 3: HP notebook, model Pavilion Entertainment dv6, with AC/DC converter, model 391174-001, (120 W), and DC/DC converter model PA-4900-OT (90 W)

The LEDs (named LED 1-3) each consisted of a converter driver and one bar (light), with the following characteristics: color temperature 4000 K, 2500 lumens, 24 V input, rated at 22 W. The AC/DC LED driver used in the AC configuration experiments used model APV-25-24. The DC configuration experiments used DC/DC driver model LDD-1000LW. The AC/DC central converter for the DC distribution configuration was an Agilent N7973A DC power supply with 0–60 VDC/0–33.3 A output, rated at 2 kW.

B. Data Collection

Each load branch in the testbed, in addition to the input and output voltage connections, were instrumented with terminal boxes to provide access to selected measurement points. Measurement data was collected using a Keysight multifunction switch measuring unit (MU) model 34980A with Keysight 34921T multiplexer and a Keysight PA2203A power analyzer. Because the MU current channels are rated up to 1 A, higher currents (up to 6 A) were measured with hall effect sensors, LEM model LTS-6-NP. The PA2203A has four dual-channel inputs, with each channel measuring current and voltage. The device can measure AC or DC signals, power consumption, power efficiency and harmonic analysis, with maximum sample rate of 5 MS/s. Its basic accuracy is 0.05% and the best power accuracy is 0.1%, both at 50/60 Hz.

Because of the number of channels needed for obtaining both voltage and current measurements on the testbed under all test configurations, and the limitation of four measurement channels on the PA2203A, data were captured at several measurement points at different instances in time after the experiments reached steady-state. The next subsection describes this process on an example configuration.

C. Configuration Example

To illustrate how the testbed was used to provide power to the loads and perform measurements during one of the configurations listed in Table I, Fig. 7 depicts the testbed under the AC-only, configuration 1 scenario.

In the configuration depicted in Fig. 7, all load branches were connected to the AC distribution bus to obtain approximate load balancing across all three phases. Input voltage and current on each phase was measured using channels 1-3 on the power analyzer (see upper left in Fig. 7). Channel 4 was used to measure voltage and current on one load branch. After capturing the load voltage and current waveforms, channel 4 was then used to obtain measurements on the remaining load branches sequentially, with channels 1-3 remaining in place. Time synchronization of all waveforms was performed during post-processing.

This report is available at no cost from the National Renewable Energy Laboratory at www.nrel.gov/publications.

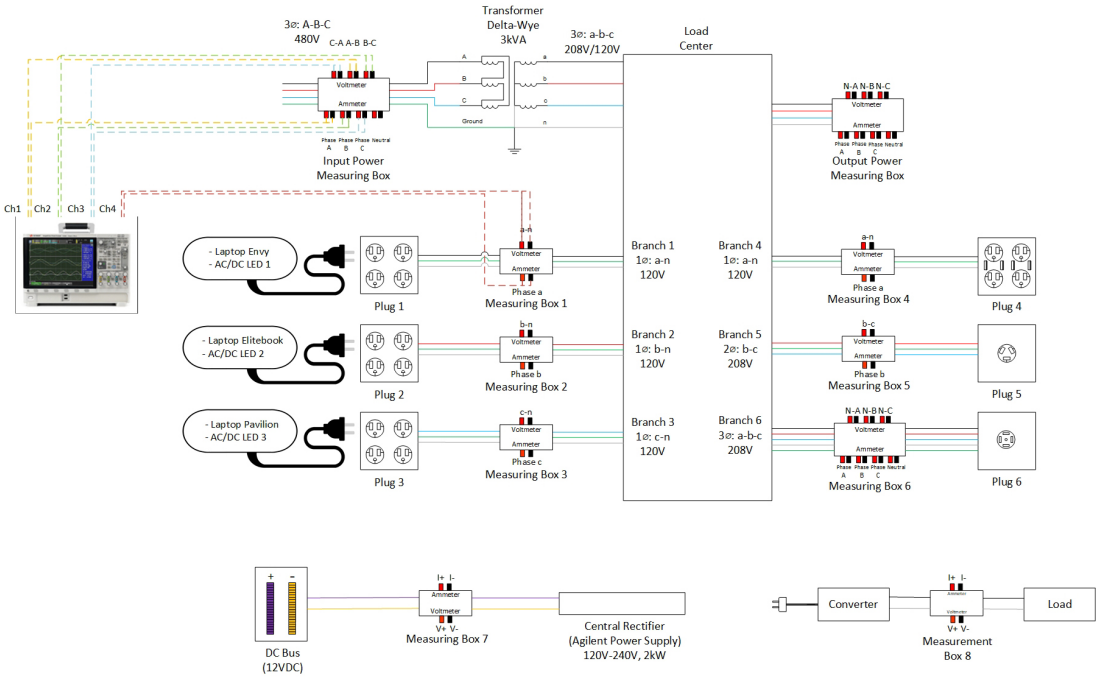

Fig. 7. Test configuration AC-only, configuration 1 (measuring phase A).

V. Model Comparisons

To evaluate the candidate models, simulations of the testbed circuit were performed for each configuration in Table I.

When applying the energy balance model, measured efficiency curves for each device in the testbed were used; all studies were performed in the Modelica® language, using the computational procedure described in [2]. The HPF model was executed in MATLAB®, using the reference impedance waveform and generalized impedance waveform representations, denoted HPF1 and HPF2, respectively. Time-domain modeling was performed in MATLAB Simscape™. Parameter values used for the time-domain studies are given in the Appendix.

The comparison of simulated system losses versus the measured reference ("Ref") values for all load configurations is shown in Fig. 8. The magnitude of error in these models versus the reference is shown in Fig. 9.

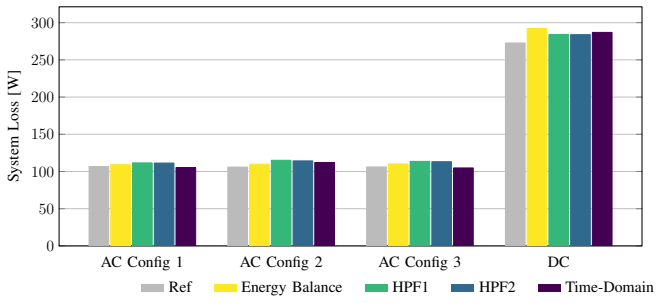

Fig. 8. Comparison of simulated losses.

As shown in Figs. 8-9, all four of the simulation models yielded similar values for system losses; however, error magnitudes varied by configuration. A breakdown of losses vs. device type under AC configuration 1 and DC configurations is shown in Figs. 10-11.

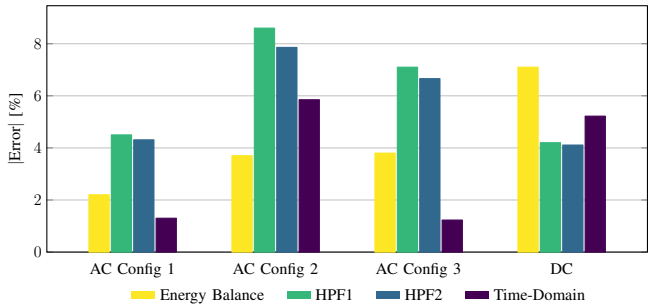

Fig. 9. Comparison of error magnitude in simulated losses.

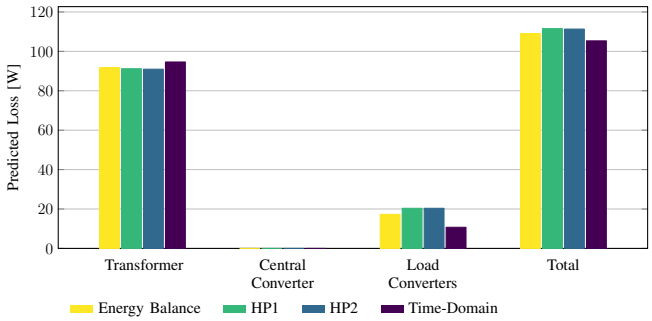

Fig. 10. Breakdown predicted losses by device type (AC Config 1).

In Fig. 10, all four of the simulation models yielded similar values and relative magnitudes for the device types, with the majority of losses occurring in the transformer (note that this configuration does not contain the central AC/DC converter). Simulations for the other AC configurations showed similar

This report is available at no cost from the National Renewable Energy Laboratory at www.nrel.gov/publications.

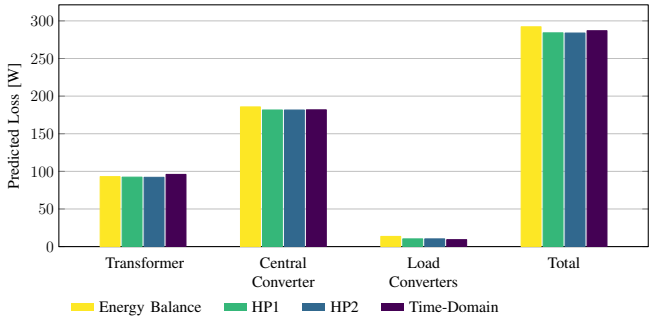

Fig. 11. Breakdown predicted losses by device type (DC Config).

results. In Fig. 11, all four of the simulation models again yielded similar values and relative magnitudes for the device types, where in this case most of the losses occurred in the central AC/DC converter, followed by the transformer, and then the load converters.

Computation times for the system simulations for each model, averaged over the AC and DC distribution configuration studies, are shown in Table II.

TABLE II. Summary of average simulation times per model.

Energy Balance	**HPF1**	**HPF2**	**Time-domain**
0.1 [s]	0.4 [s]	0.4 [s]	5.6 [s]

Discussion: As described in the simulation results above, all the candidate models yielded similar results for estimated system losses and breakdown of loss categorized by device type. The models also showed reasonably good agreement with measured reference values. In the time-domain modeling approach, further agreement could likely have been achieved through increased model fidelity, although this would have also increased computation time and modeling effort.

When comparing the candidate approaches, since all models yielded similar results, selection of the appropriate approach for implementation in a larger modeling package can therefore be made based on modeling effort, scalability, computation time, and extraction of additional features of interest (e.g., harmonic content). While the energy balance model is simple to implement, is scalable, and has low computational time, a limitation of the approach is that it cannot be used to predict harmonic content. On the other hand, the time-domain model can be used to predict harmonic content, but is the most difficult to implement, is not easily scalable, and has the highest computational cost. The HPF method provides a balance between accuracy and model development time, can be scaled to simulate large networks [14], and can also estimate harmonic content. For these reasons, the HPF model was selected for further development in future work.

VI. Conclusions

In this paper, several electrical load modeling approaches were evaluated for estimating electrical efficiencies in AC and DC distribution systems: energy balance, harmonic power flow, and time-domain modeling. These models were selected to represent a broad spectrum of expected model accuracy, computational efficiency, and implementation effort. To validate the load models under DC-only and AC-only power distribution scenarios, a testbed was constructed to provide realistic loads found in a small office building, comprising three laptop computers and three LED lighting systems on each load branch.

Based on these studies, we made the following observations on model performance: (*i*) all of the modeling approaches were found to match the experimental measurements reasonably well under AC and DC distribution, and all load configurations, (*ii*) the model results were consistent with each other in terms of how losses were distributed in each system, and (*iii*) there was an order of magnitude difference in computational time of time-domain modeling over the other methods. In terms of ease-of-implementation, the energy balance method was the easiest, time-domain modeling the most difficult, and harmonic power flow fell between these two extremes.

Overall, the harmonic power flow method was found to provide a balance between accuracy and model development time, and has the advantage of predicting harmonic content, simulation of highly unbalanced conditions, and can be scaled to simulate large networks. For these reasons, harmonic power flow was selected for further research under this effort.

Limitations of this work included the relative simplicity of the testbed circuits, simplification of the time-domain converter models, lack of non-linear loss terms and temperature effects. In addition, the central DC/DC converter was a research-grade power supply, not necessarily representative of commercial converter device efficiencies.

Suggested future research includes further validation of the harmonic power flow method on more complex network configurations and load types, and co-simulation of the electrical model with thermal models of the surrounding environment.

Acknowledgments

This work was authored in part by the National Renewable Energy Laboratory, operated by the Alliance for Sustainable Energy, LLC, for the U.S. Department of Energy (DOE) under Contract No. DE-AC36-08-GO28308, and by Lawrence Berkeley National Laboratory, operated for the DOE under Contract No. DE-AC02-05CH11231. Funding was provided by the DOE Assistant Secretary for Energy Efficiency and Renewable Energy Building Technologies Office Emerging Technologies Program. The views expressed in this article do not necessarily represent the views of the DOE or U.S. Government.

Appendix

TABLE A1. Parameters for central AC/DC converter.

Symbol	**Value**	**Symbol**	**Value**	**Symbol**	**Value**
r_1 [Ω]	0.5	C_1 [μF]	100	k_p [mV]	5.5
L_1 [μH]	10	C_2 [μF]	5	k_i [V/s]	0.89
L_2 [mH]	370	T_s [μs]	100	v_{dc}^* [V]	12

This report is available at no cost from the National Renewable Energy Laboratory at www.nrel.gov/publications.

TABLE A2. Parameters for computer (CL) and LED AC/DC converters.

Symbol	CL1	CL2	CL3	LED1	LED2	LED3
r_1 [Ω]	0.50	0.50	0.90	1.0	1.0	1.0
L_1 [μH]	10	10	10	1.0	1.0	1.0
L_2 [mH]	37	37	37	37	37	37
C_1 [μF]	100	80	100	70	70	70
C_2 [μF]	10	10	10	10	10	10
k_p [mV]	55	5.5	550	5.5	5.5	5.5
k_i [V/s]	8.86	0.89	88.6	0.89	0.89	0.89
T_s [μs]	100	10	10	10	10	10
v_{dc}^* [V]	19.5	19.5	18.6	24.2	24.2	24.2
R_L [Ω]	36	51	19.5	21	21	20

TABLE A3. Parameters for computer (CL) and LED DC/DC converters.

Symbol	CL1	CL2	CL3	LED1	LED2	LED3
L_1 [μH]	40	40	40	40	40	40
C_1 [μF]	600	600	600	600	600	600
k_p [mV]	55	55	55	55	55	55
k_i [V/s]	8.86	8.86	8.86	8.86	8.86	8.86
T_s [μs]	100	100	100	100	100	100
v_{dc}^* [V]	19.5	19.5	19.5	19.5	19.5	19.5
R_L [Ω]	35	56	17	8	8	8

TABLE A4. Parameters for AC transformer.

Description	Value
Rated apparent power	3 [kVA]
Primary voltage (line-line, rms)	480 [V]
Secondary voltage (line-line, rms)	208 [V]
Primary winding resistance	0.01 [pu]
Secondary winding resistance	0.01 [pu]
Primary leakage inductance	0.01 [pu]
Secondary leakage inductance	0.01 [pu]
Shunt magnetizing inductance	6 [pu]
Shunt magnetizing resistance	32 [pu]

REFERENCES

[1] V. Vossos, K. Garbesi, and H. Shen, "Energy savings from direct-DC in U.S. residential buildings," *Energy and Buildings*, vol. 68, pp. 223–231, Jan. 2014. [Online]. Available: http://www.sciencedirect.com/science/article/pii/S0378778813005720

[2] D. L. Gerber, V. Vossos, W. Feng, C. Marnay, B. Nordman, and R. Brown, "A simulation-based efficiency comparison of AC and DC power distribution networks in commercial buildings," *Applied Energy*, vol. 210, pp. 1167–1187, Jan. 2018. [Online]. Available: http://www.sciencedirect.com/science/article/pii/S0306261917307419

[3] S. M. Frank and S. Rebennack, "Optimal design of mixed AC-DC distribution systems for commercial buildings: A Nonconvex Generalized Benders Decomposition approach," *European Journal of Operational Research*, vol. 242, no. 3, pp. 710–729, Feb. 2015. [Online]. Available: http://www.sciencedirect.com/science/article/pii/S0377221714008121

[4] B. Glasgo, I. L. Azevedo, and C. Hendrickson, "How much electricity can we save by using direct current circuits in homes? Understanding the potential for electricity savings and assessing feasibility of a transition towards DC powered buildings," *Applied Energy*, vol. 180, pp. 66–75, Jan. 2016. [Online]. Available: http://www.sciencedirect.com/science/article/pii/S0306261916309771

[5] L. Mackay, N. H. van der Blij, L. Ramirez-Elizondo, and P. Bauer, "Toward the Universal DC Distribution System," *Electric Power Components and Systems*, vol. 45, no. 10, pp. 1032–1042, Jan. 2017. [Online]. Available: https://doi.org/10.1080/15325008.2017.1318977

[6] R. Weiss, L. Ott, and U. Boeke, "Energy efficient low-voltage DC-grids for commercial buildings," in *2015 IEEE First International Conference on DC Microgrids (ICDCM)*, 2015, pp. 154–158. [Online]. Available: http://ieeexplore.ieee.org/document/7152030/

[7] U. Boeke and M. Wendt, "DC power grids for buildings," in *2015 IEEE First International Conference on DC Microgrids (ICDCM)*, 2015, pp. 210–214. [Online]. Available: http://ieeexplore.ieee.org/document/7152040/

[8] K. Shenai and K. Shah, "Smart DC micro-grid for efficient utilization of distributed renewable energy," in *IEEE 2011 EnergyTech*, 2011, pp. 1–6. [Online]. Available: http://ieeexplore.ieee.org/document/5948505/

[9] B. A. Thomas, I. L. Azevedo, and G. Morgan, "Edison Revisited: Should we use DC circuits for lighting in commercial buildings?" *Energy Policy*, vol. 45, pp. 399–411, Jan. 2012. [Online]. Available: http://www.sciencedirect.com/science/article/pii/S0301421512001656

[10] K. Garbesi, V. Vossos, and S. Hongzia, "Catalog of DC Appliances and Power Systems," Lawrence Berkeley National Laboratories, Tech. Rep., Mar. 2011.

[11] P. Asmus and M. Lawrence, "Direct Current Distribution Networks Remote and Grid-Tied Systems for Data Center Microgrids, Telecom/Village Power, Commercial Buildings, and Military Applications: Global Market Analysis and Forecasts," Navigant Research, Tech. Rep., 2013. [Online]. Available: http://nrel.libguides.com/market/grid_utility

[12] P. Asmus and R. Elberg, "Direct Current Distribution Networks Remote and Grid-Tied Nanogrids and Microgrids for Telecom, Data Center, Commercial Building, and Military Applications," Navigant Research, Tech. Rep., 2015. [Online]. Available: http://nrel.libguides.com/market/grid_utility

[13] F. Zhang, C. Meng, Y. Yang, C. Sun, C. Ji, Y. Chen, W. Wei, H. Qiu, and G. Yang, "Advantages and challenges of DC microgrid for commercial building a case study from Xiamen university DC microgrid," in *2015 IEEE First International Conference on DC Microgrids (ICDCM)*, 2015, pp. 355–358.

[14] D. Xia and G. Heydt, "Harmonic Power Flow Studies, Part I: Formulation and Solution," *IEEE Power Engineering Review*, vol. PER-2, no. 6, pp. 17–17, Jun. 1982.

[15] D. Xia and G. Heydt, "Harmonic Power Flow Studies, Part II: Implementation and Practical Application," *IEEE Transactions on Power Apparatus and Systems*, vol. PAS-101, no. 6, pp. 1266–1270, Jun. 1982.

[16] W. Xu, J. R. Marti, and H. W. Dommel, "A multiphase harmonic load flow solution technique," *IEEE Transactions on Power Systems*, vol. 6, no. 1, pp. 174–182, Feb. 1991.

[17] W. Yifei, S. Chen, and S. S. Choi, "An overview of various approaches to power system harmonic analysis," in *2007 International Power Engineering Conference (IPEC 2007)*, Dec. 2007, pp. 338–343.

[18] N. Mohan, T. Undeland, and W. Robbins, *Power Electronics: Converters, Applications, and Design, 2nd ed.* Hoboken, NJ: Wiley, IEEE Press, 2013.

[19] P. Krause, O. Wasynczuk, S. Sudhoff, and S. Pekarek, *Analysis of Electric Machinery and Drive Systems, 3rd ed.* Hoboken, NJ: Wiley, IEEE Press, 2013.

[20] J. D. Glover, M. S. S. Sarma, and T. Overbye, *Power System Analysis and Design, 4th ed.* Stamford, CT: Cengage Learning, 2008.

[21] D. King, G. Gonzalez, M. Galbraith, and W. Boyson, "Performance Model for Grid-Connected Photovoltaic Inverters," Sandia National Laboratories, Tech. Rep., Sep. 2007.

[22] D. Fregosi, S. Ravula, D. Brhlik, J. Saussele, S. Frank, E. Bonnema, J. Scheib, and E. Wilson, "A comparative study of DC and AC microgrids in commercial buildings across different climates and operating profiles," in *2015 IEEE First International Conference on DC Microgrids (ICDCM)*, 2015, pp. 159–164.

[23] U. Eminoglu and M. Hocaoglu, "Distribution Systems Forward/Backward Sweep-based Power Flow Algorithms: A Review and Comparison Study," *Electric Power Components and Systems*, vol. 37, no. 1, pp. 91–110, 2008.

This report is available at no cost from the National Renewable Energy Laboratory at www.nrel.gov/publications.